Supplementary Materials:

Materials and Methods

Supplementary Text

Figures S1-S6

Tables S1-S4

References (*42*-*54*)

Materials and Methods

Equatorial Atlantic Intermediate / Deep Water (EAI/DW) coral sampling

The fossil coral samples of EAI/DW were collected in situ using a Remotely Operated Vehicle (ROV) during the RRS *James Cook* Cruise JC094, from October 2013 – November 2013 in the northern Equatorial Atlantic from five locations: Carter Seamount (EBA, eastern basin, 9.2°N, 21.3°W), Knipovich Seamount (EBB, eastern basin, 5.6°N, 26.9°W), Vema Fracture Zone (VEM, western basin, 10.7°N, 44.6°W), Vayda Seamount (VAY, western basin, 14.9°N, 48.2°W) and Gramberg Seamount (GRM, western basin, 15.4°N, 51.1°W). The samples reported here have a water-depth range between 750-2814 m. They are classified into 5 layers by the water depth: shallowest (750-845 m), shallow (972-1162 m), middle (1296-1492 m), deep (1545-1612 m), and deepest (1827-2100 m). A single sample was from 2814 m and was not taken into account for the classification. From our cruise data, the low salinity core in the water columns which indicates the depth of Antarctic Intermediate Water (AAIW) advection is ~700-800 m, whereas the maximum salinity (34.95-35.0) composed of North Atlantic Deep Water (NADW) is located at a depth of ~1500 m in both the eastern and western basins. In the modern, the shallowest layer is more influenced by AAIW compared with other layers, whereas the deep layer is dominated by influence from NADW and the deepest layer by influence from the deep ocean mixing between NADW and Antarctic Bottom Water (AABW).

Sample selection and reconnaissance dating

More than 2000 fossil solitary scleractinian corals and 85 kg of fossil colonial scleractinian corals were recovered during the JC094 cruise (details are available in (*42*)). Solitary scleractinian corals including 580 *Caryophyllia*, 50 *Desmophyllum*, 54 *Javania*, 7

Dasmosmillia, 3 *Polymyces* and colonial scleractinian corals including 85 pieces of *Enallopsammia*, 11 pieces of *Madrepora*, 12 pieces of *Solenosmilia*, have been reconnaissance dated applying the laser-ablation U-Th reconnaissance method recently developed in our lab, which has a precision of <2 ka for samples < 40 ka. Most of the coral samples selected for reconnaissance dating are well preserved, with minimal internal bio-erosion, except *Desmophyllum* which shows internal bio-erosion features such as micro-boring holes in the coral septa. In total 800 reconnaissance ages were obtained. Seventy samples were selected for further study including 41 *Caryophyllia*, 15 *Enallopsammia*, 5 *Solenosmilia*, 4 *Desmophyllum*, 4 *Madrepora*, 1 *Polymyces* (Table S1).

U-series dating

Approximately 0.2 gram of each coral sample was cut and the ferromanganese and organic coatings or re-calcified parts were carefully removed with a Dremel tool, with additional chemical cleaning to remove any residual contaminants (*9*).

The procedure involving column chemistry and mass spectrometry for U-series dating on deep-sea corals follows previously well-developed methods (*9, 13, 17, 43*). Briefly, cleaned coral aragonite was dissolved in 7 M optima-grade HNO_3 and spiked with ~ 0.06 g of the ^{236}U-^{229}Th mixed spike which has been calibrated to a 2σ uncertainty of about 4‰ in other studies (*13*). U and Th in the carbonates were first co-precipitated with iron hydroxides and then extracted by centrifugation. Anion-exchange columns were used to further separate and purify U and Th fractions. U and Th isotopes were measured by bracketing standards (international U standard: U112a; and in house Th standard: SGS) on a Neptune Multi-Collected Inductively-Coupled-Plasma Mass Spectrometer (MC-ICP-MS) in the Bristol Isotope Group at the University of Bristol. Before each session of measurement, the machine accuracy and precision was checked by repeatedly measuring U (HU1) and Th (ThB) standards. Monitoring of machine stability using the same standards was also carried out every 3 to 4 samples during measurements. The typical internal precision for $^{234}U/^{238}U$ is ~0.7-1‰ and for $^{229}Th/^{230}Th$ is ~0.9-1.5‰, with accuracy better than 1‰ and 2‰ respectively. The isotopes ^{229}Th, ^{230}Th were measured on the secondary electron multiplier (SEM) by peak jumping. To avoid the influence of signal instability during peak jumping between ^{229}Th and ^{230}Th, we needed another isotope that could be simultaneously measured on a Faraday cup for normalizing purpose. Because clean coral can have particularly low ^{232}Th, a pure ^{236}U spike was added to the Th fraction which allows ^{236}U to be measured on a

Faraday cup. This spike does not affect the Th isotope system but provides a way for normalizing $^{229}Th/^{230}Th$ by measuring $^{229}Th/^{236}U$ and $^{230}Th/^{236}U$ (*13*).

Full procedural blanks and the Harwell uraninite standard (HU1) were processed in each session of column chemistry. The Harwell uraninite standard (HU1) gave a long-term external reproducibility of [$^{230}Th/^{230}U$] (activity ratio) of 2.8‰ (n=9, 2 S.D.) within error of secular equilibrium, which is better than the calculated error for individual measurement (5-6‰). The reason that the final individual errors are larger is partly because they include other sources of uncertainties such as spike calibration (4 ‰). For sample uncertainty calculations we considered an additional source of uncertainty (Fig. S6b), the initial ^{230}Th in the coral, which is estimated assuming an initial atomic $^{232}Th/^{230}Th$ ratio of 12,500 ± 12,500 (2σ) (*17*), typical of the modern subtropical Atlantic intermediate waters. To calculate the coral age, errors including machine and procedural blanks are first propagated analytically into the isotope ratios of $^{234}U/^{238}U$, $^{236}U/^{238}U$, $^{229}Th/^{230}Th$. We then applied a Monte Carlo technique (resolving the U-series age equation (*44*) 100,000 times for each sample using random numbers generated within the error uncertainty of each variable) to propagate the errors of isotope ratios into the final uncertainties.

The final age uncertainty is significantly correlated with the ^{232}Th concentration (i.e., higher ^{232}Th means higher uncertainty of initial ^{230}Th activity), so efforts were made to duplicate samples to get the lowest ^{232}Th possible. The duplicate sample results were always within error of each other. In our final data set we reject ages which had U-series age uncertainties that are >350 years to minimize the uncertainty on the final radiocarbon reconstruction. The relative age deviations of 13 pairs of duplicate samples (uncertainty less than 350 years) measured during the course of U-series dating were typically (10 out of 13) less than 6‰ (full range between 0.2‰ and 10.7‰). For corals that have duplicates, the calendar ages of the sample with lowest ^{232}Th concentration was used for calculation of radiocarbon parameters (see below). Calculated initial $\delta^{234}U_i$ of EAI/DW corals ($\delta^{234}U_i$ is the deviation from secular equilibrium in ‰ units of the $^{234}U/^{238}U$ activity ratio incorporated into the coral skeleton during coral growth) in this study (Fig. S6a) range from 142.5-152.7‰ with an average value of 147.8 ± 3.9‰ (2 S.D.). We assume these coral skeletons are in a closed system given their initial $\delta^{234}U$ are all within 7‰ of the modern day ocean (146.7 ‰ (*44-46*)).

<u>Radiocarbon analysis and calculation of $\Delta^{14}C$, $\Delta\Delta^{14}C$, and the B-Atmosphere age</u>

The corals with well-constrained U-Th ages were analyzed for radiocarbon at the UC Irvine Keck-CCAMS facility in two analytical sessions. Approximately 20 mg of each sample was taken from the oxidative-cleaned coral samples (*47*). Prior to acid dissolution by concentrated phosphoric acid in vacuumed 5 ml tubes, these samples were first leached by 0.1 N HCl to remove any adsorbed CO_2 (*47*). Around 50% of total mass was removed during this stage. Graphitization of CO_2 was done on a hydrogen reduction vacuum line in the AMS lab of University of California Irvine. The $^{14}C/^{12}C$ and $^{13}C/^{12}C$ of the graphite were measured on the UC Irvine Keck-CCAMS facility. Three ^{14}C dead samples (2 *Caryophyllia* and 1 *Desmophyllum*) from the JC094 cruise, with ages from 145 ka to 268 ka, were used as blanks, which give fraction modern (Fm) of 0.0019 ± 0.0012 (n = 14, 2 S.D.) without notable correlation with species or age. The Fraction Modern of the ^{14}C data reported in Table S2 were blank-corrected based on measurements of these ^{14}C-dead coral samples. Note that the blank of our study is lower by a factor of two than previously reported coral ^{14}C blanks (*13, 17, 48*).

There are a number of ways to present paleo-^{14}C data, as recently described in detail by (*49*). The $\Delta^{14}C$ (or known-age radiocarbon correction) is useful for showing how the signature of the past seawater evolves with time and is calculated as: $\Delta^{14}C_{coral} = (Fm \times e^{(calender\ age/8267)} - 1) \times 1000$. However given the changing atmospheric $\Delta^{14}C$, it is useful to present the offset of seawater $\Delta^{14}C$ from the contemporary atmosphere using $\Delta\Delta^{14}C$. The $\Delta\Delta^{14}C$ is calculated as $\Delta^{14}C_{coral} - \Delta^{14}C_{atmosphere}$. It is also important to account for the change in ^{14}C inventory over time to allow for direct comparison of radiocarbon data between time periods (*13, 49*). A useful parameter for this comparison is the B-Atmosphere age, which is calculated as the radiocarbon age difference between the ocean (coral, R_{cora}) and the contemporary atmosphere ($R_{atmosphere}$). B-Atmosphere age accounts for the effects of the changing atmospheric ^{14}C inventory which can cause hidden biases when interpreting $\Delta\Delta^{14}C$ data (*13, 49*). Both $\Delta^{14}C_{atmosphere}$ and $R_{atmosphere}$ are taken from IntCal13 calibration curve in this study (*12*).

We applied a Monte Carlo technique to propagate the uncertainties of atmosphere ^{14}C into our calculations. This propagation was done by generating random numbers constrained by the coral calendar-age uncertainties and using the corresponding $\Delta^{14}C_{atmosphere}$ and $R_{atmosphere}$, as well as the associated uncertainties in the IntCal13 calibration curve. Error ellipses were calculated accordingly based on the random-data distribution in the calendar age versus $\Delta^{14}C_{coral}$, calendar age versus $\Delta\Delta^{14}C$ and calendar age versus $\Delta^{14}C_{coral}$ coordinate spaces for each sample.

Supplementary Text

Radiocarbon in the Equatorial Atlantic seawater and recent corals

At location EBB, the $\Delta^{14}C$ of the seawater is -94‰ to -103‰ from 800-1000 m depth (Fig. S2), while two *Caryophyllia* samples with ages of 267 and 733 years at depth of 749 and 845 m have $\Delta^{14}C$ of -111‰, -109‰, respectively. At VEM station, $\Delta^{14}C$ of the seawater is -88‰ at 1204 m depth (Fig. S2), while one *Madrepora* sample with an age of 372 years at depth of 1296 m has a $\Delta^{14}C$ of -84‰ and one *Caryophyllia* sample with an age of 474 years at a depth of 1327 m has a $\Delta^{14}C$ of -88‰. At VAY station, $\Delta^{14}C$ of the seawater is -91‰ at 1607 m depth (nearby GLODAP bottle data, Fig. S2) (*14*), while one *Enallopsammia* sample with an age of 692 years at a depth of 1612 m has a $\Delta^{14}C$ of -94‰. These results add further confidence to the finding that modern-collected corals reflect the radiocarbon of dissolved inorganic carbon (*50*).

Equatorial Atlantic LGM coral with high $\Delta^{14}C$

The $\Delta^{14}C$ of an LGM *Solenosmilia* sample (f0115solnm002a, 22.3 ka) is similar to the contemporary atmosphere (Fig. S3, Table S2), an unexpected result given that another coral with the same U-series age (f0115solnm002f, 22.3 ka) from the same site yield $\Delta^{14}C$ values some 180‰ lower. It is possible that the high $\Delta^{14}C$ of this *Solenosmilia* sample could be related to a rapid ventilation event of the Equatorial Atlantic intermediate waters at around 22.3 ka. However without more data to confirm this ^{14}C-enriched signature or other evidence to support the existence of this rapid ventilation event, our argument remains speculative and therefore the ^{14}C result of this *Solenosmilia* sample is not included for discussion in the main text.

Equatorial Atlantic corals: east to west

In our discussion, we have not separated the west basin records from the east basin records, as any difference between the two sides of the basin are thought to be minimal for our discussion: (1) the modern seawater ^{14}C profile is similar between the east and west basins above 2100 m water depth (Fig. S2); (2) there is no major geographical barrier between the east and west basin above 2100 m water depth, enabling the chemical tracers to mix rapidly along isopycnal surfaces in the past and the modern time; (3) the major shift of ^{14}C signature in each period is generally characterized by data from the same basin, rather than mixed basin signals (Fig. S5).

New ^{14}C data from the Drake Passage

Compared with the 31-point published ^{14}C dataset (*13*) we have now increased the resolution of the Southern Ocean record by 24 with sampling effort mainly in the LGM and the early B-A interstadial from corals collected by dredge on cruise NBP11-03 in the Drake Passage. All samples were from the depth window which in the modern day is filled by Upper Circumpolar Deep Water (UCDW). The sampling and U-series/^{14}C dating follows the previous study and methods outlined above (*13*) and the new record of UCDW is included as a complementary dataset (Table S3, S4) for our study.

Larger ^{14}C gradients in the glacial ocean

As described in detail in (*51, 52*), glacial shoaling of the interface between NADW and AABW may have resulted in reduced diapycnal mixing between these two water masses and a greater expansion of the less-ventilated AABW in the abyssal ocean. Inverse modeling on the distribution of LGM nutrient proxies, however, shows NADW might still contribute a large fraction of the deep Atlantic waters (*53*). The results of (*53*) imply a much reduced deep-advection rate which would facilitate respired carbon storage in the deep water, consistent with ^{14}C depleted signatures. Hence the increased glacial deep-ocean ^{14}C stratification suggests a dominant control by vertical reorganization of deep-water mass distribution and/or slower advection rate at depth (*51, 53*). On the other hand, the larger $\Delta^{14}C$ difference that we observed between glacial EAI/DW and UCDW represents a latitudinal gradient (Fig. 2C). UCDW in the modern day is a mixture of NCW and AABW, so the enhanced spatial ^{14}C gradient within the upper ocean at the LGM was likely to be due to a lower $\Delta^{14}C$ signature of the AABW (end-member change) and/or a lower mixing of NCW into the UCDW.

Comparison of foraminifera and coral records on AMOC 'overshoot' during the B-A

The ^{14}C record of (*16*) showed a better ventilated abyssal South Atlantic (4981 m) throughout B-A than the modern, pointing to the possibility of an AMOC overshoot lasting more than one thousand years. However the resolution of their record was not high enough to resolve centennial events in the early B-A. Moreover, bioturbation in sediment cores could potentially smooth out centennial events, making them appear longer lived. Some records such as the reconstructed [CO_3^{2-}] concentration in the southwest Pacific deep water (*36)* and magnetic susceptibility of a northwest Atlantic sediment core *(54*) did record short-lived events that were consistent with AMOC overshooting at the start of B-A, but determining the

absolute duration of these events in sediment cores is difficult. In addition, modeling simulations suggest that the interior deep ocean may be less sensitive to the centennial scale overshoot events (*37*). With our high-resolution record, we have the ability to precisely detect the timing of the overshoot events in the Drake Passage, which suggests it lasted only 400-500 years. It is, however, possible that the Drake Passage record is not well placed to record the continued AMOC overshoot (i.e. the AMOC could have been still stronger than the modern, but its influence in the Drake Passage was much reduced). We do not have coral data available to constrain whether the Drake Passage ^{14}C (UCDW) quickly returned to a well ventilated condition after the initial decline at about 14.1 ka, so we cannot rule out a subsequent return to strengthened AMOC conditions.

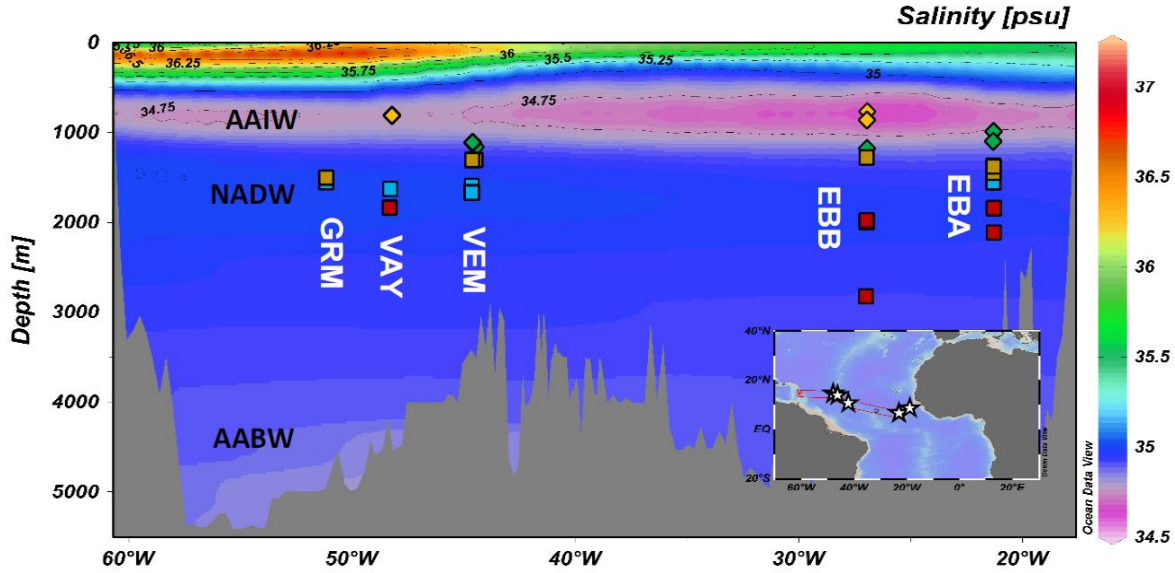

Fig. S1. Longitude-depth distribution of the sampling locations superimposed on the salinity sections of the northern Equatorial Atlantic (WOCE09). White stars in the lower right map mark the geographical location of the five seamounts (from left to right: GRM (Gramberg Seamount), VAY (Vayda Seamount), VEM (Vema fracture Zone), EBB (Knipovich Seamount), and EBA (Carter Seamount)) where coral samples were collected.

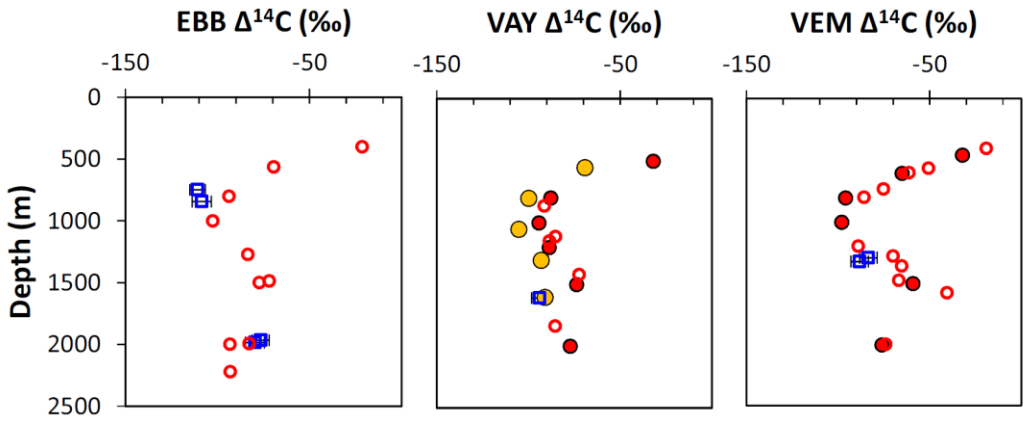

Fig. S2. Comparison between late Holocene (<2.5 ka) Equatorial Atlantic Intermediate / Deep water coral ^{14}C data (unfilled blue squares) and modern seawater profiles. JC094 cruise CTD data and ROV data are represented by unfilled and filled red circles, respectively. Nearby GLODAP data (*14*) are represented by filled yellow circles.

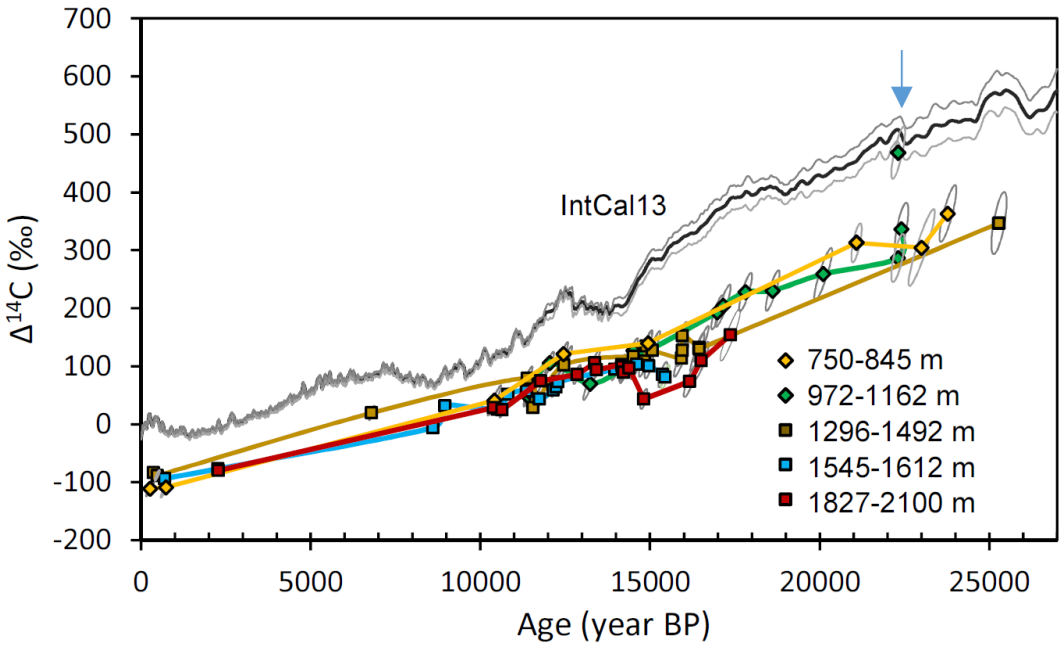

Fig. S3. $\Delta^{14}C$ with 2σ error ellipses of all Equatorial Atlantic Intermediate / Deep water coral data. Blue arrow indicates the data point not included for discussion.

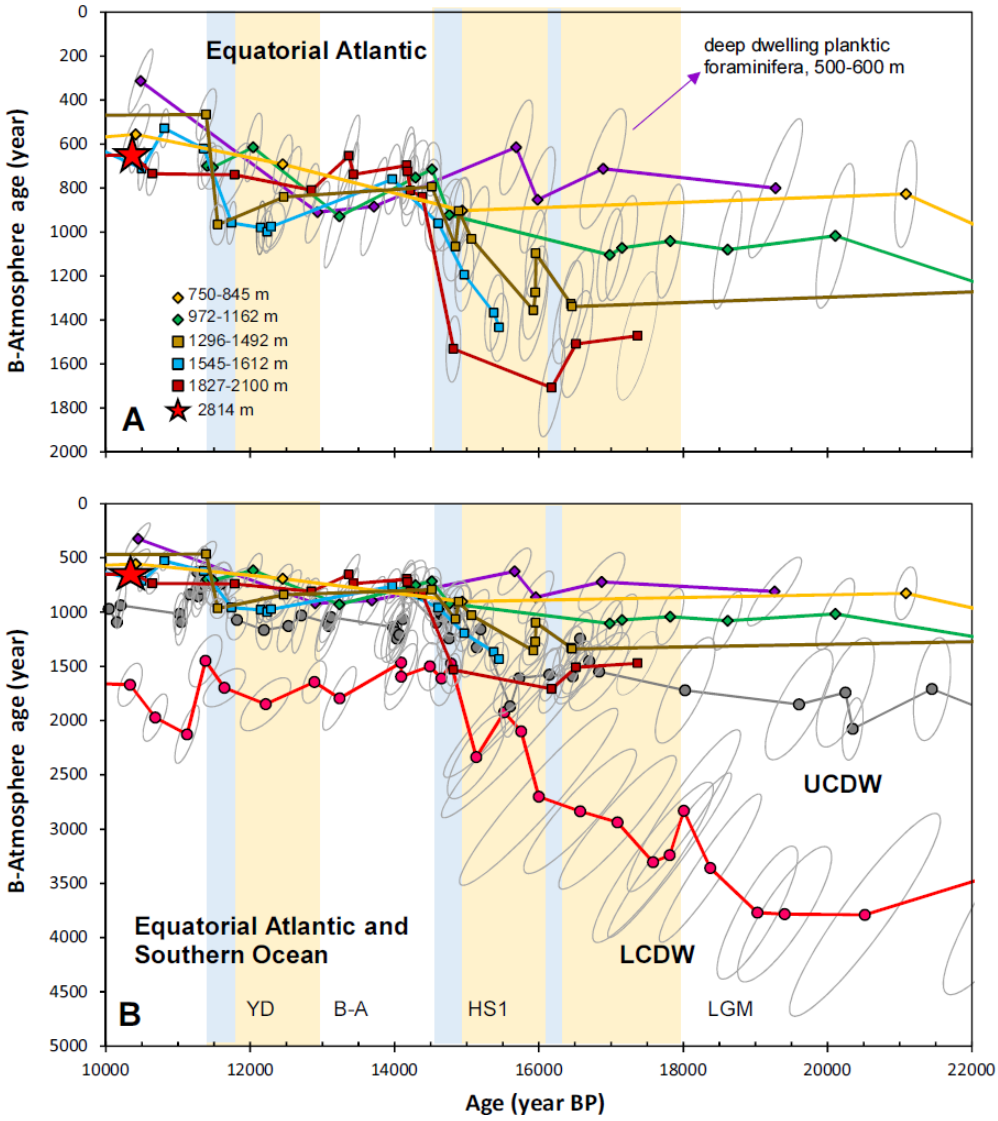

Fig. S4. (**A**) Comparison of B-Atmosphere ages of Equatorial Atlantic Intermediate / Deep water corals with Equatorial Atlantic deep dwelling foraminifera-atmosphere ^{14}C ages (*21*) recalculated based on IntCal13 (*12*) during the last deglaciation. (**B**) Comparison of B-Atmosphere ages between Equatorial Atlantic records, Upper Circumpolar Deep Water (UCDW) (*13*) and Lower Circumpolar Deep Water (LCDW, Benthic foraminifera-atmosphere ^{14}C age, (*18*)) from the Southern Ocean, based on IntCal13 (*12*). The age model of LCDW is based on the published Bchron calendar age (*18*).

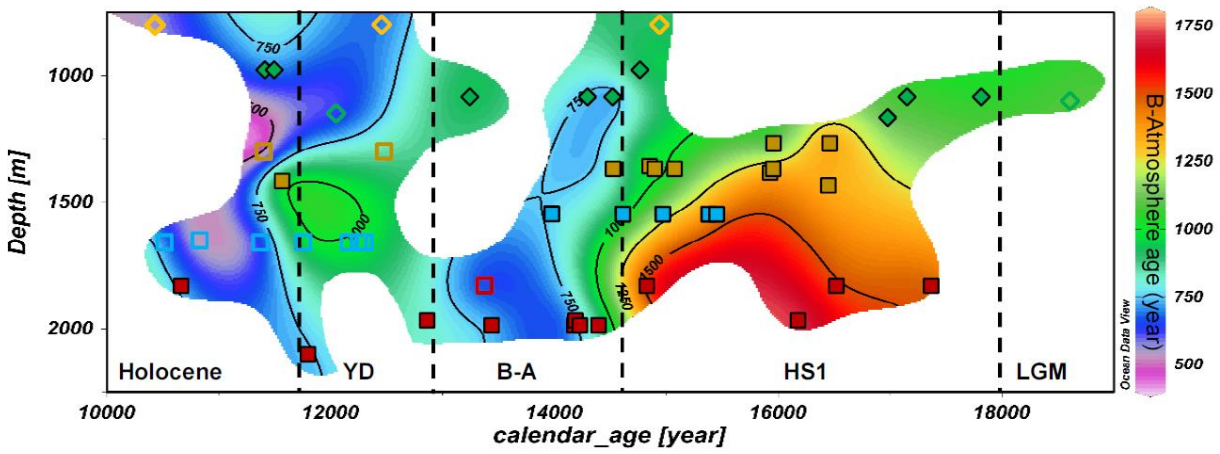

Fig. S5. Age-depth distribution of the Equatorial Atlantic Intermediate / Deep water coral samples (19-10 ka) reported in this study. The underlying colour map shows the B-Atmosphere age evolution of EAI/DW during the last deglaciation. Note the samples of YD are mainly from the western basin (unfilled), while the samples of HS1 and B-A are mainly from the eastern basin (filled).

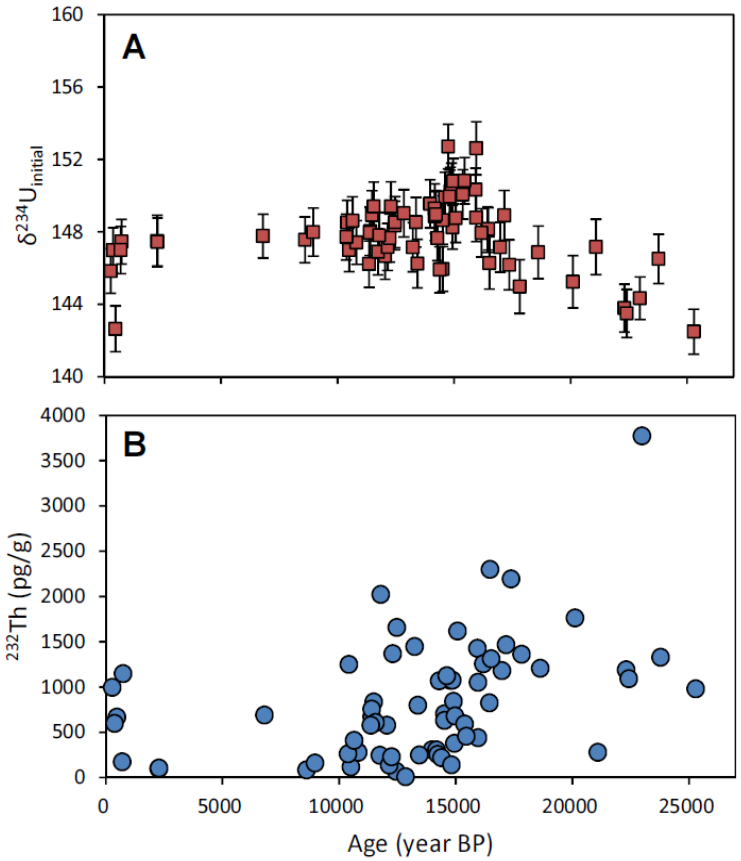

Fig. S6. Calculated initial $\delta^{234}U_i$ (**A**) and ^{232}Th concentration (**B**) of the Equatorial Atlantic Intermediate / Deep water coral samples versus their calendar ages. Error bars of ^{232}Th concentration are smaller than the symbols. Note the $\delta^{234}U_{initial}$ evolution appears to be consistent with the prediction of (*45*).

Table S1. Uranium series dating on deep-sea corals from the Equatorial Atlantic.

Sample	Group	*Genus*	Age (year) after ini. ^{230}Th corr.	2 σ	Age (year) before ini. ^{230}Th corr.	2 σ	$\delta^{234}U_m$	2 σ	$\delta^{234}U_i$	2 σ	^{238}U (ppm)	2 σ	^{232}Th (ppt)	2 σ	$^{230}Th/^{238}U$ activity ratio	2 σ
f0079carcs002	A	*Caryophyllia*	333	99	431	3	145.9	1.2	145.8	1.2	4.68	0.01	998	4.2	0.0045	3.2E-05
f0076carcs001	A	*Caryophyllia*	795	128	923	10	147.3	1.2	147.5	1.2	4.14	0.01	1148	5.3	0.0097	1.1E-04
f0186carcs002	A	*Caryophyllia*	10,477	160	10,625	61	144.3	1.2	148.5	1.2	3.89	0.01	1251	5.6	0.1063	5.7E-04
f0186carcs004	A	*Caryophyllia*	12,514	111	12,583	88	143.4	1.3	148.4	1.3	0.46	0.00	69	0.3	0.1247	8.1E-04
f0186descm001	A	*Desmophyllum*	15,001	101	15,042	92	142.2	1.2	148.3	1.2	4.21	0.01	378	2.0	0.1474	8.2E-04
f0076carcs011	A	*Caryophyllia*	21,153	126	21,188	121	138.9	1.5	147.2	1.5	3.73	0.01	281	1.4	0.2015	1.0E-03
f0186carcs005	A	*Caryophyllia*	23,044	349	23,366	131	135.3	1.1	144.3	1.2	5.41	0.01	3776	16.6	0.2195	1.1E-03
duplicate sample			23,070	315	23,347	151	135.4	1.3	144.2	1.4	3.63	0.01	2179	10.5	0.2194	1.3E-03
f0076carcs002	A	*Caryophyllia*	23,845	205	23,975	159	137.2	1.3	146.5	1.4	4.73	0.01	1330	7.0	0.2250	1.3E-03
f0052carcsm036L	B	*Caryophyllia*	11,463	104	11,545	65	143.7	1.3	148.0	1.3	3.79	0.01	673	3.0	0.1149	6.0E-04
f0052carcsm037L	B	*Caryophyllia*	11,546	133	11,663	64	144.8	1.3	148.9	1.3	3.32	0.01	835	3.7	0.1161	5.9E-04
f0123descm001	B	*Desmophyllum*	12,106	102	12,176	76	141.9	1.2	146.7	1.3	3.85	0.01	580	3.1	0.1207	7.0E-04

f0001carcs005	B	*Caryophyllia*	13,298	164	13,446	69	141.8	1.3	147.2	1.4	4.49	0.01	1448	6.0	0.1326	6.2E-04
f0001carcs012	B	*Caryophyllia*	14,348	153	14,472	88	142.0	1.2	147.7	1.3	3.97	0.01	1069	5.2	0.1421	7.9E-04
f0001descm008	B	*Desmophyllum*	14,580	104	14,651	76	140.2	1.2	146.0	1.2	4.57	0.01	703	3.0	0.1435	6.8E-04
f0052carcsm041L	B	*Caryophyllia*	14,817	161	14,954	84	146.6	1.2	152.7	1.2	3.60	0.01	1075	4.6	0.1471	7.6E-04
f0094descm005	B	*Desmophyllum*	17,044	144	17,158	87	140.5	1.3	147.2	1.4	4.77	0.01	1182	4.9	0.1663	7.6E-04
duplicate sample			17,163	255	17,394	111	139.0	1.3	145.8	1.3	4.66	0.01	2323	12.0	0.1682	9.7E-04
f0001carcs066	B	*Caryophyllia*	17,215	179	17,363	101	142.2	1.3	148.9	1.4	4.58	0.01	1466	6.2	0.1684	8.9E-04
f0001carcs058	B	*Caryophyllia*	17,882	156	18,011	89	138.0	1.4	145.0	1.5	4.90	0.01	1362	5.6	0.1735	7.6E-04
f0115solnm002d	B	*Solenosmilia*	18,680	165	18,805	110	140.1	1.4	146.9	1.5	4.49	0.01	1208	5.2	0.1808	9.4E-04
f0115solnm002c	B	*Solenosmilia*	20,169	213	20,338	131	138.0	1.4	145.2	1.4	4.83	0.01	1764	7.1	0.1939	1.1E-03
f0115solnm002f	B	*Solenosmilia*	22,372	168	22,470	136	135.6	1.2	143.8	1.3	5.59	0.01	1190	5.0	0.2119	1.1E-03
f0115solnm002b	B	*Solenosmilia*	22,479	161	22,573	131	135.2	1.3	143.5	1.3	5.40	0.01	1092	4.6	0.2127	1.1E-03
f0137madnsml001	C	*Madrepora*	435	58	493	2	147.6	1.2	147.0	1.2	4.75	0.01	597	1.8	0.0052	2.2E-05
f0107carnm001	C	*Caryophyllia*	538	60	598	2	142.5	1.3	142.6	1.3	5.16	0.01	668	1.6	0.0062	2.1E-05
f0228madnm001	C	*Madrepora*	6,863	69	6,925	32	146.2	1.2	147.8	1.2	5.15	0.01	692	2.5	0.0704	3.0E-04
f0108carcs003	C	*Caryophyllia*	11,455	115	11,547	70	143.6	1.4	148.0	1.4	3.81	0.01	756	3.8	0.1150	6.5E-04
f0029polcm001	C	*Polymyces*	11,616	88	11,679	62	145.1	1.3	149.4	1.3	4.45	0.01	610	2.6	0.1163	5.7E-04
f0108carcs001	C	*Caryophyllia*	12,529	196	12,708	76	143.5	1.4	148.5	1.4	4.26	0.01	1659	7.8	0.1259	7.0E-04
f0047carcs023	C	*Caryophyllia*	14,579	113	14,643	93	142.8	1.3	148.7	1.3	4.54	0.01	632	3.4	0.1438	8.4E-04
f0059carcs002	C	*Caryophyllia*	14,910	144	15,021	91	144.2	1.3	150.2	1.3	4.48	0.01	1076	4.8	0.1474	8.2E-04
f0047carcs021	C	*Caryophyllia*	14,959	141	15,062	95	144.6	1.4	150.4	1.4	3.73	0.01	842	3.8	0.1478	8.5E-04
f0047carcs026	C	*Caryophyllia*	15,135	189	15,305	85	142.6	1.3	148.8	1.4	4.40	0.01	1620	7.1	0.1498	7.6E-04
f0031carcm002	C	*Caryophyllia*	15,988	173	16,134	92	143.9	1.1	150.3	1.2	4.49	0.01	1429	5.9	0.1575	8.2E-04
f0048carcs003	C	*Caryophyllia*	16,016	144	16,127	92	142.3	1.3	148.8	1.3	4.40	0.01	1053	4.7	0.1573	8.2E-04
duplicate sample			15,846	217	16,042	93	143.3	1.2	149.7	1.3	4.85	0.01	2066	8.5	0.1566	8.3E-04
f0073carcs002	C	*Caryophyllia*	16,020	119	16,078	105	146.3	1.4	152.6	1.5	3.51	0.01	442	2.5	0.1573	9.3E-04
f0027carns013	C	*Caryophyllia*	16,508	132	16,601	94	141.6	1.2	148.1	1.3	4.09	0.01	825	3.5	0.1614	8.3E-04
f0073carcs001	C	*Caryophyllia*	16,529	227	16,738	90	141.5	1.1	148.2	1.2	5.06	0.01	2299	9.5	0.1627	8.0E-04
duplicate sample			16,602	227	16,808	99	141.1	1.2	147.7	1.3	5.23	0.01	2330	10.6	0.1632	8.7E-04
f0047carcsm001	C	*Caryophyllia*	25,352	174	25,458	138	133.5	1.2	142.5	1.2	4.32	0.01	981	4.1	0.2365	1.1E-03
f0218enansml001	D	*Enallopsammia*	756	17	773	3	147.7	1.3	147.0	1.3	4.82	0.01	175	0.6	0.0081	3.2E-05
f0160enansm001f	D	*Enallopsammia*	8,666	35	8,674	34	145.2	1.2	147.6	1.3	4.71	0.01	84	0.5	0.0875	3.2E-04
f0163enacsm001a	D	*Enallopsammia*	9,026	37	9,042	33	145.4	1.3	148.0	1.3	4.58	0.01	160	0.5	0.0911	3.0E-04
f0160enapsm001b	D	*Enallopsammia*	10,563	44	10,575	43	143.6	1.2	147.0	1.2	4.48	0.01	119	0.5	0.1057	3.9E-04
f0161enacsm001c	D	*Enallopsammia*	10,876	50	10,902	43	144.6	1.2	147.4	1.2	5.01	0.01	279	1.0	0.1088	3.9E-04
f0160enapsm001d	D	*Enallopsammia*	11,421	68	11,480	32	143.9	1.2	146.2	1.3	4.46	0.01	578	1.4	0.1142	2.8E-04
f0160enansm001d	D	*Enallopsammia*	11,807	53	11,833	46	143.7	1.2	146.9	1.3	4.28	0.01	245	0.9	0.1175	4.2E-04
f0160enapsm001c	D	*Enallopsammia*	12,213	51	12,227	50	143.0	1.3	147.2	1.3	4.48	0.01	138	0.5	0.1213	4.4E-04
f0160enansm001a	D	*Enallopsammia*	12,303	57	12,329	50	143.3	1.3	147.7	1.3	3.99	0.01	229	0.7	0.1223	4.5E-04
f0160enansm001e	D	*Enallopsammia*	12,356	150	12,488	70	144.5	1.3	149.4	1.4	4.77	0.01	1367	5.8	0.1239	6.5E-04
f0255enansm001	D	*Enallopsammia*	14,036	93	14,067	87	143.9	1.3	149.6	1.3	4.59	0.01	307	1.4	0.1386	7.9E-04
f0021madQnm001b	D	*Madrepora?*	14,675	148	14,784	99	143.9	1.3	149.9	1.4	4.74	0.02	1124	4.8	0.1452	8.9E-04
f0021madQnm001a	D	*Madrepora?*	15,033	105	15,101	80	144.8	1.2	150.8	1.3	4.61	0.01	682	2.9	0.1482	7.2E-04
f0021enacm001a	D	*Enallopsammia*	15,442	107	15,502	88	144.0	1.3	150.1	1.4	4.53	0.01	593	2.6	0.1518	7.9E-04
f0021enacm001b	D	*Enallopsammia*	15,514	103	15,566	89	144.6	1.2	150.8	1.3	4.03	0.01	456	2.0	0.1524	8.0E-04
f0061carnm010	E	*Caryophyllia*	2,331	23	2,343	19	146.7	1.4	147.5	1.4	3.87	0.01	97	1.9	0.0243	2.0E-04

f0060carnm013	E	*Caryophyllia*	2,337	21	2,349	18	146.6	1.3	147.4	1.3	4.18	0.01	105	1.3	0.0244	1.8E-04
f0083carnm001	E	*Caryophyllia*	10,447	49	10,471	42	144.1	1.2	147.7	1.3	4.92	0.01	263	0.8	0.1047	3.9E-04
f0019enacm004b	E	*Enallopsammia*	10,711	69	10,749	57	144.7	1.3	148.6	1.3	4.97	0.01	410	1.8	0.1075	5.3E-04
f0042carcs002	E	*Caryophyllia*	11,850	182	12,014	78	143.1	1.2	147.8	1.3	5.68	0.02	2022	10.1	0.1193	7.2E-04
f0061carnm009	E	*Caryophyllia*	12,914	85	12,926	84	143.9	1.3	149.0	1.3	0.40	0.00	11	0.1	0.1280	7.7E-04
f0211carcs001	E	*Caryophyllia*	13,432	123	13,513	93	143.2	1.3	148.5	1.4	4.57	0.01	798	4.1	0.1334	8.5E-04
f0060carnm002	E	*Caryophyllia*	13,494	58	13,519	52	140.8	1.3	146.2	1.3	4.50	0.01	249	0.8	0.1332	4.6E-04
f0060carnm007	E	*Caryophyllia*	14,237	86	14,268	81	143.5	1.3	149.3	1.4	4.48	0.01	300	1.4	0.1404	7.3E-04
f0061carnm005	E	*Caryophyllia*	14,242	90	14,274	84	143.1	1.3	148.9	1.3	4.42	0.01	305	1.5	0.1404	7.6E-04
f0060carnm012	E	*Caryophyllia*	14,286	95	14,313	91	143.2	1.3	149.0	1.3	4.45	0.01	258	1.4	0.1408	8.3E-04
f0060carnm005	E	*Caryophyllia*	14,453	55	14,476	51	140.1	1.2	145.9	1.3	4.49	0.01	221	0.6	0.1419	4.4E-04
f0019enacm004a	E	*Enallopsammia*	14,881	85	14,897	83	143.8	1.4	149.9	1.5	3.94	0.01	142	0.8	0.1462	7.4E-04
f0061carnm037	E	*Caryophyllia*	16,239	148	16,356	89	141.4	1.3	147.9	1.3	4.94	0.01	1258	5.4	0.1592	7.9E-04
duplicate sample			16,236	211	16,420	103	141.4	1.4	147.8	1.4	4.90	0.01	1960	8.3	0.1598	9.1E-04
f0019carns012	E	*Caryophyllia*	16,585	174	16,718	112	139.7	1.4	146.3	1.5	4.52	0.01	1314	6.7	0.1622	9.9E-04
duplicate sample			16,537	236	16,749	100	141.3	1.3	147.9	1.3	4.59	0.01	2116	10.1	0.1627	8.9E-04
f0019carns015	E	*Caryophyllia*	17,430	236	17,643	103	139.3	1.3	146.2	1.4	4.77	0.01	2194	9.9	0.1705	8.9E-04
f0115solnm002a	B	*Solenosmilia*	22,385	164	22,486	127	135.8	1.3	144.0	1.4	5.20	0.01	1140	4.8	0.2120	1.1E-03

* Group A to E corresponds to the depth range of samples of 750-845 m, 972-1162 m, 1296-1492 m, 1546-1612 m, 1827-2100 m, respectively.

Table S2. Calendar age and radiocarbon data of deep-sea corals from the Equatorial Atlantic.

sample	Location	Latitude (°N)	Longitude (°E)	Group	Depth (m)	Calendar age (year BP)	2 σ	Fraction Modern (blank corrected)	2 σ	$\Delta^{14}C$ (‰)	$\Delta\Delta^{14}C$ (‰)	B-Atmosphere (year)
f0079carcs002	EBB	5.627	-26.947	A	749	267	99	0.8608	0.0033	-111	-119	1004
f0076carcs001	EBB	5.626	-26.950	A	845	733	128	0.8157	0.0039	-109	-96	826
f0186carcs002	VAY	14.890	-48.153	A	795	10414	160	0.2954	0.0018	41	-75	556
f0186carcs004	VAY	14.890	-48.153	A	795	12449	111	0.2488	0.0015	122	-101	692
f0186descm001	VAY	14.890	-48.153	A	795	14938	101	0.1871	0.0014	140	-136	903
f0076carcs011	EBB	5.626	-26.950	A	845	21088	126	0.1024	0.0015	313	-142	827
f0186carcs005	VAY	14.890	-48.153	A	795	23008	315	0.0807	0.0013	305	-192	1110
f0076carcs002	EBB	5.626	-26.950	A	845	23781	205	0.0768	0.0012	364	-156	871
f0052carcsm036L	EBA	9.220	-21.310	B	973	11400	104	0.2641	0.0017	49	-95	700
f0052carcsm037L	EBA	9.220	-21.310	B	973	11480	133	0.2630	0.0019	55	-97	706
f0123descm001	VEM	10.727	-44.424	B	1146	12039	102	0.2578	0.0017	106	-88	615
f0001carcs005	EBA	9.216	-21.316	B	1080	13234	164	0.2159	0.0017	70	-131	929
f0001carcs012	EBA	9.216	-21.316	B	1080	14289	153	0.1956	0.0015	102	-108	752
f0001descm008	EBA	9.216	-21.316	B	1080	14516	104	0.1948	0.0015	128	-105	714
f0052carcsm041L	EBA	9.220	-21.310	B	973	14759	161	0.1882	0.0016	122	-136	922
f0094descm005	EBB	5.620	-26.959	B	1162	16980	144	0.1530	0.0016	193	-176	1104
f0001carcs066	EBA	9.216	-21.316	B	1080	17153	179	0.1512	0.0016	205	-171	1073
f0001carcs058	EBA	9.216	-21.316	B	1080	17818	156	0.1423	0.0016	228	-170	1042
f0115solnm002d	VEM	10.742	-44.558	B	1097	18614	165	0.1295	0.0015	231	-178	1081
f0115solnm002c	VEM	10.742	-44.558	B	1097	20106	213	0.1106	0.0015	259	-170	1018
f0115solnm002f	VEM	10.742	-44.558	B	1097	22311	168	0.0866	0.0015	287	-218	1257
f0115solnm002b	VEM	10.742	-44.558	B	1097	22414	161	0.0888	0.0017	337	-161	914
f0137madnsml001	VEM	10.729	-44.425	C	1296	372	58	0.8762	0.0037	-84	-87	731
f0107carnm001	VEM	10.741	-44.569	C	1327	474	60	0.8610	0.0032	-88	-97	815
f0228madnm001	GRM	15.422	-51.087	C	1492	6798	69	0.4480	0.0022	20	-62	476
f0108carcs003	VEM	10.741	-44.567	C	1296	11391	115	0.2721	0.0017	79	-64	466
f0029polcm001	EBA	9.206	-21.298	C	1413	11552	88	0.2543	0.0018	29	-132	967
f0108carcs001	VEM	10.741	-44.567	C	1296	12468	196	0.2439	0.0018	102	-121	841
f0047carcs023	EBA	9.207	-21.300	C	1366	14516	113	0.1929	0.0016	117	-116	794
f0059carcs002	EBA	9.205	-21.299	C	1354	14846	144	0.1840	0.0017	108	-157	1067
f0047carcs021	EBA	9.207	-21.300	C	1366	14893	141	0.1873	0.0016	135	-136	906
f0047carcs026	EBA	9.207	-21.300	C	1366	15069	189	0.1821	0.0016	127	-155	1032
f0031carcm002	EBA	9.206	-21.298	C	1380	15925	173	0.1623	0.0016	114	-206	1357
f0048carcs003	EBA	9.208	-21.301	C	1365	15952	144	0.1637	0.0017	127	-194	1275
f0073carcs002	EBB	5.625	-26.966	C	1264	15955	119	0.1673	0.0016	153	-168	1098
f0027carns013	EBA	9.206	-21.297	C	1431	16446	132	0.1549	0.0015	133	-204	1328
f0073carcs001	EBB	5.625	-26.966	C	1264	16458	227	0.1544	0.0014	130	-207	1340
f0047carcsm001	EBA	9.207	-21.300	C	1366	25287	174	0.0632	0.0015	347	-224	1233
f0218enansml001	VAY	14.865	-48.256	D	1612	692	17	0.8334	0.0034	-94	-80	681
f0160enansm001f	VEM	10.755	-44.602	D	1657	8602	35	0.3512	0.0017	-6	-74	574
f0163enacsm001a	VEM	10.753	-44.602	D	1578	8962	37	0.3489	0.0021	32	-64	479
f0160enapsm001b	VEM	10.755	-44.602	D	1657	10499	44	0.2881	0.0018	26	-95	712

f0161enacsm001c	VEM	10.754	-44.603	D	1648	10813	50	0.2843	0.0017	52	-71	529
f0160enapsm001d	VEM	10.755	-44.602	D	1657	11358	68	0.2675	0.0020	57	-85	621
f0160enansm001d	VEM	10.755	-44.602	D	1657	11742	53	0.2521	0.0018	43	-133	959
f0160enapsm001c	VEM	10.755	-44.602	D	1657	12149	51	0.2436	0.0017	59	-138	981
f0160enansm001a	VEM	10.755	-44.602	D	1657	12238	57	0.2422	0.0017	64	-141	1000
f0160enansm001e	VEM	10.755	-44.602	D	1657	12291	150	0.2427	0.0017	73	-139	976
f0255enansm001	GRM	15.422	-51.086	D	1544	13972	93	0.2020	0.0017	95	-109	761
f0021madQnm001b	EBA	9.203	-21.293	D	1545	14609	148	0.1885	0.0015	103	-140	961
f0021madQnm001a	EBA	9.203	-21.293	D	1545	14967	105	0.1801	0.0018	101	-177	1195
f0021enacm001a	EBA	9.203	-21.293	D	1545	15378	107	0.1690	0.0016	86	-202	1368
f0021enacm001b	EBA	9.203	-21.293	D	1545	15451	103	0.1669	0.0016	82	-212	1434
f0061carnm010	EBB	5.602	-26.966	E	1966	2267	23	0.7020	0.0029	-77	-78	652
f0060carnm013	EBB	5.602	-26.967	E	1985	2273	21	0.6992	0.0031	-80	-83	688
f0083carnm001	EBB	5.589	-26.994	E	2814	10382	49	0.2929	0.0017	28	-87	650
f0019enacm004b	EBA	9.199	-21.289	E	1829	10646	69	0.2827	0.0017	25	-99	735
f0042carcs002	EBA	9.197	-21.284	E	2100	11785	182	0.2583	0.0017	75	-103	740
f0061carnm009	EBB	5.602	-26.966	E	1966	12850	85	0.2295	0.0016	86	-115	809
f0211carcs001	VAY	14.858	-48.257	E	1827	13369	123	0.2195	0.0016	106	-94	654
f0060carnm002	EBB	5.602	-26.967	E	1985	13429	58	0.2156	0.0015	94	-106	738
f0060carnm007	EBB	5.602	-26.967	E	1985	14172	86	0.1987	0.0014	103	-100	697
f0061carnm005	EBB	5.602	-26.966	E	1966	14180	90	0.1978	0.0015	99	-104	725
f0060carnm012	EBB	5.602	-26.967	E	1985	14221	95	0.1950	0.0014	89	-115	812
f0060carnm005	EBB	5.602	-26.967	E	1985	14388	55	0.1924	0.0017	97	-121	840
f0019enacm004a	EBA	9.199	-21.289	E	1829	14819	84	0.1738	0.0016	44	-219	1533
f0061carnm037	EBB	5.602	-26.966	E	1966	16176	148	0.1517	0.0016	74	-254	1708
f0019carns012	EBA	9.199	-21.289	E	1829	16517	174	0.1505	0.0016	110	-231	1510
f0019carns015	EBA	9.199	-21.289	E	1829	17367	236	0.1412	0.0018	154	-232	1472
f0115solnm002a	VEM	10.742	-44.558	B	1097	22316	164	0.0987	0.0015	467	-37	187

* Group A to E corresponds to the depth range of samples of 750-845 m, 972-1162 m, 1296-1492 m, 1546-1612 m, 1827-2100 m, respectively.

Table S3. Uranium series dating on deep-sea corals from the Drake Passage

Sample	*Genus*	Age (year) after ini. ^{230}Th corr.	2 σ	Age (year) before ini. ^{230}Th corr.	2 σ	$\delta^{234}U_m$	2 σ	$\delta^{234}U_i$	2 σ	^{238}U (ppm)	2 σ	^{232}Th (ppt)	2 σ	^{230}Th/^{238}U activity ratio	2 σ
NBP1103-DH120-Dc-25	*Desmophyllum*	12,626	124	12,782	66	143.1	0.4	148.3	0.4	3.76	0.01	509	2.1	0.1266	5.8E-04
NBP1103-DH120-Dn-01	*Desmophyllum*	13,175	131	13,338	72	142.2	0.4	147.6	0.4	5.02	0.01	710	3.0	0.1316	6.3E-04
NBP1103-DH120-Dn-01	*Desmophyllum*	13,220	134	13,391	70	142.5	0.4	148.0	0.4	5.07	0.01	753	3.1	0.1322	6.0E-04
NBP1103-DH16-Bc-2	*Balanophyllia*	14,073	206	14,211	183	141.6	4.6	147.4	4.9	4.61	0.01	552	3.6	0.1397	1.1E-03
NBP1103-DH120-Dc-33	*Desmophyllum*	14,113	162	14,229	141	141.2	4.4	146.9	4.7	4.26	0.01	430	2.1	0.1398	7.4E-04
NBP1103-DH120-Dc-21	*Desmophyllum*	14,125	121	14,266	76	142.9	0.4	148.7	0.4	4.05	0.01	494	2.1	0.1403	6.5E-04
NBP1103-DH120-Dc-21	*Desmophyllum*	14,165	115	14,295	74	143.2	0.4	149.1	0.4	4.05	0.01	456	1.9	0.1406	6.4E-04
NBP1103-DH117-Dn-7	*Desmophyllum*	14,205	162	14,319	143	146.0	4.5	152.0	4.7	3.66	0.01	363	1.7	0.1412	7.5E-04
NBP1103-DH117-Dc-20	*Desmophyllum*	14,239	243	14,583	78	146.0	0.4	152.0	0.5	3.47	0.01	1041	4.3	0.1436	6.7E-04
NBP1103-DH117-Dc-29b	*Desmophyllum*	14,671	148	14,754	137	145.0	4.1	151.2	4.3	4.20	0.01	305	1.4	0.1451	7.3E-04
NBP1103-DH74-Dc-3	*Desmophyllum*	14,776	244	15,062	152	145.2	4.5	151.4	4.8	3.82	0.01	950	4.5	0.1479	7.9E-04
NBP1103-DH120-Dc-32	*Desmophyllum*	14,845	131	15,001	78	141.6	0.4	147.7	0.4	3.98	0.01	538	2.3	0.1469	6.7E-04
NBP1103-DH117-Dc-36	*Desmophyllum*	14,951	159	15,032	149	147.5	4.3	153.9	4.6	3.67	0.01	260	1.4	0.1480	8.0E-04
NBP1103-DH88- Cc-1	*Caryophyllia*	15,232	176	15,373	148	138.5	4.1	144.6	4.4	3.62	0.01	440	2.7	0.1499	7.9E-04
NBP1103-DH75-Dc(f)-37	*Desmophyllum*	15,283	145	15,460	83	142.1	0.4	148.3	0.4	4.35	0.01	668	2.9	0.1512	7.1E-04
NBP1103-DH19-Fc-01	*Flabellum*	15,823	289	16,232	91	142.1	0.4	148.6	0.5	2.80	0.01	994	4.3	0.1582	7.6E-04
NBP1103-DH75-Gc-4	*Gardeneria*	16,238	115	16,345	89	140.4	0.4	147.0	0.4	6.06	0.01	563	2.7	0.1590	7.6E-04
NBP1103-DH117-Dc-9	*Desmophyllum*	16,913	336	17,347	169	139.7	4.2	146.5	4.5	4.73	0.01	1773	8.2	0.1679	8.8E-04
NBP1103-DH40-Dc-3	*Desmophyllum*	18,109	337	18,532	182	142.5	4.2	150.0	4.6	3.67	0.01	1346	6.6	0.1789	9.3E-04
NBP1103-DH43-Dc-6	*Desmophyllum*	19,693	378	20,166	206	135.8	4.4	143.5	4.8	3.34	0.01	1362	6.7	0.1922	1.0E-03
NBP1103-DH43-Dc-1	*Desmophyllum*	20,429	116	20,462	113	136.5	0.4	144.6	0.4	5.68	0.01	162	1.8	0.1949	9.2E-04
NBP1103-DH40-Dc-5	*Desmophyllum*	22,640	162	22,788	127	135.9	0.4	144.9	0.5	2.99	0.01	383	1.6	0.2148	1.0E-03
NBP1103-DH75-Gc-3	*Gardeneria*	25,958	218	26,192	151	135.3	0.4	145.6	0.5	5.17	0.01	1046	4.5	0.2432	1.2E-03
NBP1103-DH43-Dc-3	*Desmophyllum*	27,221	244	27,505	152	135.8	0.4	146.7	0.5	3.21	0.01	790	3.3	0.2541	1.2E-03

Table S4. Calendar age and radiocarbon data of deep-sea corals from the Drake Passage

sample	Location	Latitude (°S)	Longitude (°W)	Depth (m)	Calendar age (year BP)	2 σ	Fraction Modern (blank corrected)	2 σ	Δ14C (‰)	ΔΔ14C (‰)	B-Atmosphere (year)
NBP1103-DH120-Dc-25	Sars Seamount	59 47.91	68 57.62	1701	12564	124	0.2328	0.0034	64	-161	1132
NBP1103-DH120-Dn-01	Sars Seamount	59 47.91	68 57.62	1701	13113	131	0.2147	0.0025	49	-155	1104
NBP1103-DH120-Dn-01	Sars Seamount	59 47.91	68 57.62	1701	13158	134	0.2147	0.0013	54	-147	1051
NBP1103-DH16-Bc-2	Burdwood Bank	54 48.52	62 07.20	1419	14011	206	0.1915	0.0034	42	-160	1141
NBP1103-DH120-Dc-33	Sars Seamount	59 47.91	68 57.62	1701	14051	162	0.1899	0.0034	40	-164	1188
NBP1103-DH120-Dc-21	Sars Seamount	59 47.91	68 57.62	1701	14063	121	0.1881	0.0027	31	-174	1247
NBP1103-DH120-Dc-21	Sars Seamount	59 47.91	68 57.62	1701	14103	115	0.1881	0.0027	36	-168	1213
NBP1103-DH117-Dn-7	Sars Seamount	59 45.82	68 56.00	981	14143	162	0.1905	0.0031	54	-151	1070
NBP1103-DH117-Dc-20	Sars Seamount	59 45.82	68 56.00	981	14177	243	0.1961	0.0027	89	-117	819
NBP1103-DH117-Dc-29b	Sars Seamount	59 45.82	68 56.00	981	14609	148	0.1852	0.0031	85	-159	1102
NBP1103-DH74-Dc-3	Interim Seamount	60 36.33	66 00.13	1064	14714	244	0.1852	0.0031	98	-156	1065
NBP1103-DH120-Dc-32	Sars Seamount	59 47.91	68 57.62	1701	14783	131	0.1804	0.0024	79	-181	1245
NBP1103-DH117-Dc-36	Sars Seamount	59 45.82	68 56.00	981	14889	159	0.1870	0.0031	133	-137	921
NBP1103-DH88- Cc-1	Interim Seamount	60 33.75	65 57.40	983	15170	176	0.1737	0.0024	88	-196	1330
NBP1103-DH75-Dc(f)-37	Interim Seamount	60 36.00	66 00.00	1196	15221	145	0.1763	0.0025	111	-173	1161
NBP1103-DH19-Fc-01	Burdwood Bank	54 48.57	62 10.02	1516	15761	289	0.1597	0.0026	75	-238	1612
NBP1103-DH75-Gc-4	Interim Seamount	60 36.00	66 00.00	1196	16176	115	0.1543	0.0026	92	-237	1579
NBP1103-DH117-Dc-9	Sars Seamount	59 45.82	68 56.00	981	16851	336	0.1460	0.0029	121	-240	1551
NBP1103-DH40-Dc-3	Shackleton Fracture Zone	60 10.90	57 50.00	806	18047	337	0.1272	0.0033	128	-271	1723
NBP1103-DH43-Dc-6	Shackleton Fracture Zone	60 10.90	57 50.00	823	19631	378	0.1048	0.0029	126	-293	1852
NBP1103-DH43-Dc-1	Shackleton Fracture Zone	60 10.90	57 50.00	823	20367	116	0.0944	0.0021	109	-329	2078
NBP1103-DH40-Dc-5	Shackleton Fracture Zone	60 10.90	57 50.00	806	22578	162	0.0755	0.0020	158	-328	2003
NBP1103-DH75-Gc-3	Interim Seamount	60 36.00	66 00.00	1196	25896	218	0.0536	0.0022	231	-322	1866
NBP1103-DH43-Dc-3	Shackleton Fracture Zone	60 10.90	57 50.00	823	27159	244	0.0448	0.0019	198	-372	2167

Supplementary References

42. L. F. Robinson, "RRS James Cook Cruise JC094, October 13–November 30 2013, Tenerife-Trinidad. TROPICS, Tracing Oceanic Processes using Corals and Sediments. Reconstructing abrupt Changes in Chemistry and Circulation of the Equatorial Atlantic Ocean: Implications for global Climate and deep-water Habitats.," (University of Bristol, 2014).
43. M. E. Auro *et al.*, Improvements to 232-thorium, 230-thorium, and 231-protactinium analysis in seawater arising from GEOTRACES intercalibration. *Limnol. Oceanogr.-Meth.* **10**, 464-474 (2012).
44. R. Edwards, C. Gallup, H. Cheng, Uranium-series dating of marine and lacustrine carbonates. *Rev. Mineral. Geochem.* **52**, 363-405 (2003).
45. L. F. Robinson, G. M. Henderson, L. Hall, I. Matthews, Climatic control of riverine and Seawater uranium-isotope ratios. *Science* **305**, 851-854 (2004).
46. P. J. Reimer *et al.*, Intcal09 and Marine09 Radiocarbon Age Calibration Curves, 0-50,000 Years Cal Bp. *Radiocarbon* **51**, 1111-1150 (2009).
47. J. F. Adkins *et al.*, Radiocarbon dating of deep-sea corals. *Radiocarbon* **44**, 567-580 (2002).
48. S. F. Eltgroth, J. F. Adkins, L. F. Robinson, J. Southon, M. Kashgarian, A deep-sea coral record of North Atlantic radiocarbon through the Younger Dryas: Evidence for intermediate water/deepwater reorganization. *Paleoceanography* **21**, (2006).

49. M. S. Cook, L. D. Keigwin, Radiocarbon profiles of the NW Pacific from the LGM and deglaciation: Evaluating ventilation metrics and the effect of uncertain surface reservoir ages. *Paleoceanography*, 2014PA002649 (2015).
50. J. F. Adkins, H. Cheng, E. A. Boyle, E. R. M. Druffel, R. L. Edwards, Deep-Sea Coral Evidence for Rapid Change in Ventilation of the Deep North Atlantic 15,400 Years Ago. *Science* **280**, 725-728 (1998).
51. J. F. Adkins, The role of deep ocean circulation in setting glacial climates. *Paleoceanography* **28**, 539-561 (2013).
52. R. Ferrari *et al.*, Antarctic sea ice control on ocean circulation in present and glacial climates. *Proc. Natl. Acad. Sci. U.S.A.* **111**, 8753-8758 (2014).
53. G. Gebbie, How much did Glacial North Atlantic Water shoal? *Paleoceanography* **29**, 190-209 (2014).
54. J. D. Stanford *et al.*, Timing of meltwater pulse 1a and climate responses to meltwater injections. *Paleoceanography* **21**, (2006).